Parameter analysis for the design of statically balanced serial linkages using a stiffness matrix approach with Cartesian coordinates

Herder, Just; Lustig, M.P.; Dunning, Gerard

DOI
10.6567/IFToMM.14TH.WC.PS3.008

Publication date
2015

Document Version
Final published version

Published in
Proceedings of the 14th IFToMM World Congress

The 14th IFToMM World Congress, Taipei, Taiwan, October 25-30, 2015
DOI Number: 10.6567/IFToMM.14TH.WC.PS3.008

Parameter analysis for the design of statically balanced serial linkages using a stiffness matrix approach with Cartesian coordinates

M. P. Lustig*
Delft University of Technology
Delft, The Netherlands

A. G. Dunning†
Delft University of Technology
Delft, The Netherlands

J. L. Herder‡
Delft University of Technology
Delft, The Netherlands

Abstract—*A statically balanced system is in equilibrium in every pose. In classical balancing solutions for serial linkages, each DOF is balanced by an independent element. Disadvantages are increased mass and inertia for counter-mass, and auxiliary links for spring solutions. Recent literature presents a method for balancing serial linkages without auxiliary links; using multi-articular springs. This method obtains constraint equations from the stiffness matrix. Downsides are different coordinate systems for describing locations and states, and criteria constraining attachments to fixed lines In the present paper Cartesian coordinates are implemented in the stiffness matrix approach. Goal is comparing the use of this single coordinate system to using multiple, and obtaining increased insight in and providing a visualization of parameter relations. The Cartesian coordinates are implemented, providing a simple, intuitive method for designing statically balanced serial linkages allowing for recognition of the full design space. Obtained parameter relations are visualized in an example.*

Keywords: Static balance, Zero-free-length spring, Serial linkage

I. Introduction

A system which is in equilibrium in every motionless state is called statically balanced. For such systems the potential energy level remains constant in every pose [1]. This constant energy level greatly reduces operational effort as only dynamic effects remain to be overcome during motion. Many applications for static balancing exist due to these benefits [1], [2], [3], [4].

Different techniques exist to statically balance the rotation of a rigid pendulum. A simple option is adding a counter-mass [1], downside of which is the increased mass and inertia [5]. A second option is connecting a zero-free-length spring (ZFLS) between the link and fixed world [1]. For a ZFLS the spring force is proportional to its length. Other less common solutions use a non-circular cam [6] or compliant flexure elements [7]. These solutions are all designed to balance a single degree of freedom (DOF).

Solutions for balancing a serial linkage with multiple DOF make use of counter-mass or ZFLSs. In the first case a counter-mass is added to each link [8], [9], additional auxiliary links allow counter-mass relocation [10]. Inertia increase becomes a greater problem as added weights of distal counter-masses must be balanced as well. Classical ZFLS solutions require a parallel beam construction providing a link with fixed orientation at each joint [1], [11], [12]. Each link is balanced by a single ZFLS that spans the joint of the respective link, a mono-articular spring. The disadvantage of parallel beams are an increased complexity and added inertia. In these systems each DOF is balanced by an independent balancing element.

Recent literature presents two methods in which ZFLSs can span multiple joints to balance serial linkages without parallel beams. The first method is the stiffness matrix approach by Lin et al. [12], [13], [14], [15]. Energy equations are set up in a general form $U = \frac{1}{2}\boldsymbol{Q}^T\boldsymbol{K}\boldsymbol{Q}$, separating states $\boldsymbol{Q}$ and parameters in a stiffness matrix $\boldsymbol{K}$. Off-diagonal elements of $\boldsymbol{K}$ contain state dependent energy terms, constraining these terms equal to zero results in a statically balanced system [13]. The second method is an iterative method developed by Deepak and Ananthasuresh [16]. Balance is ensured link by link, in steps, starting at the most distal link. At each step, balance of a specific link is acquired by adding up to two ZFLSs between this link and fixed world. For each link only energy terms of the current and previous step links affect its constraint equations [16]. In these two methods each DOF is balanced by combined efforts of multiple ZFLSs.

Both methods can create statically balanced serial linkages and are based on an energy approach. Nevertheless multiple differences exist in ease of implementation and capabilities. The first is that in Lin's method all constraints are obtained at once for a chosen spring configuration, whereas in Deepak's method only a selection of the constraints is evaluated at once. If no straightforward solution is found, Deepak's method explains which spring(s) can be added for a solvable system, Lin's method does not directly. However, information on which links are unbalanced and thus require additional springs can be extracted from the stiffness matrix [15]. Another difference is that all springs are connected to the fixed world in Deepak's method while in Lin's method springs can be attached in between any two links, i.e. additional constraints are provided considering these springs. Finally, Deepak's method allows pla-

*M.P.Lustig@student.tudelft.nl
†A.G.Dunning@tudelft.nl
‡J.L.Herder@tudelft.nl

nar placement of spring attachments while in Lin's method criteria are set up constraining attachments to be located on fixed straight lines [15].

In the presented work the stiffness matrix approach is selected for calculating balanced linkages as it provides all constraints at once and allows additional spring placement options. The exact implementation however is altered. Current literature describes locations on links using polar coordinate systems, while states are described using unit vectors (xy-components). In the presented work Carthesian (xy-) coordinates are used describing link locations as well as the states.

Three goals are formulated in the presented paper. The first goal is to implement Cartesian coordinates in the stiffness matrix approach for balanced serial linkages to investigate its benefits over the combined use of polar coordinates for locations and xy-coordinates for states. The second goal is to gain more insight in the relations between different parameters of this method in the design space, for instance it will be investigated if placement of springs outside the vertical straight lines is allowed. The third goal is to visualize these behavioral relations in an example.

The structure of this paper is as follows. First, in 'Method' the Cartesian coordinate stiffness matrix approach is derived. Next, in 'Application and behavior' the example of a balanced linkages is presented of which the behavior is analyzed. Third, in 'Discussion' the use of Cartesian and polar coordinates are compared. Finishing with the obtained conclusions concerning the set goals.

II. Method

We propose the consistent use of Cartesian coordinates in the stiffness matrix approach for designing serial statically balanced linkages. This is in contrast to the use of polar coordinates for locations and Cartesian coordinates for states, as used in current literature on this method [12], [13], [14], [15]. In the presented paper the location of spring attachments, joints and COMs is described using (local) x- and y- coordinates on the respective links they are located on. In this section the assumptions are explained first, followed by the full derivation of the stiffness matrix approach using xy-coordinates.

A. Assumptions and limitations

The presented method is set up for planar linkages, the gravitational field acting in this plane has constant magnitude and direction. The links are connected to each other and/or the fixed world using revolute joints. All springs have linear ZFLS behavior and the mass of these springs is neglected. Mechanical limits of links/springs colliding with one another are not taken into account. The fixed world is assumed to be rigid and static.

B. Derivation of stiffness matrix

The stiffness matrix approach is derived in five steps. First all coordinate points are described as a function of the link states and parameter values. The second step is setting up potential energy equations for all spring and mass components and writing these equations in a generalized form. The third step is to combine the energy equations of the different components to obtain the total stiffness matrix. The fourth step is obtaining the constraint equations for balance from the stiffness matrix. The fifth and final step is focused on how to solve the obtained equations. The equations are set up for an n link system where the fixed world is link 1, as a result the system has $n-1$ moving links.

B.1 Step 1: Coordinate vectors

The state of link u is described by global unit vector $\boldsymbol{q}_u$ (Figure 1a). The fixed world vector $\boldsymbol{q}_1$ is constant, aligned with the global x-axis. For moving links ($u = 2 \cdots n$) vector $\boldsymbol{q}_u$ is aligned with the local x_u-axis. The origin of each local coordinate system is located at the proximal joint J_{u-1}. The y_u-axis are orientated perpendicular to the respective x_u-axis. A unit vector in this y_u direction is obtained by rotating the state vector $\boldsymbol{q}_u$ by 90° using rotation matrix $\boldsymbol{R}$. Combined state vector $\boldsymbol{Q}$ holds the states of all n-links.

$$\boldsymbol{q}_1 = \begin{bmatrix} 1 \\ 0 \end{bmatrix} \tag{1a}$$

$$\boldsymbol{q}_u = \begin{bmatrix} q_{xu} \\ q_{yu} \end{bmatrix} \tag{1b}$$

$$\boldsymbol{Q} = \begin{bmatrix} \boldsymbol{q}_1 \\ \vdots \\ \boldsymbol{q}_n \end{bmatrix} \tag{1c}$$

$$\boldsymbol{I} = \begin{bmatrix} 1 & 0 \\ 0 & 1 \end{bmatrix} \tag{1d}$$

$$\boldsymbol{R} = \begin{bmatrix} \cos(90^\circ) & -\sin(90^\circ) \\ \sin(90^\circ) & \cos(90^\circ) \end{bmatrix} = \begin{bmatrix} 0 & -1 \\ 1 & 0 \end{bmatrix} \tag{1e}$$

Global coordinates of all point on the links are described as a linear combination of the state vectors and constant parameter values. Joint locations are described first. As said, fixed world joint $\boldsymbol{J}_1$ is located in the global origin. The distal joint $\boldsymbol{J}_u$ of a link u is always located on the local x_u-axis at distance L_u from the local origin (Figure 1b). Vector components of joint locations are set up in equation 2.

$$\boldsymbol{J}_1 = \begin{bmatrix} 0 \\ 0 \end{bmatrix} \tag{2a}$$

$$\begin{aligned} \boldsymbol{J}_u &= L_2\boldsymbol{I}\boldsymbol{q}_2 + L_3\boldsymbol{I}\boldsymbol{q}_3 + \cdots + L_u\boldsymbol{I}\boldsymbol{q}_u \\ &= \sum_{i=2}^{u} L_i\boldsymbol{I}\boldsymbol{q}_i = \boldsymbol{J}_{u-1} + L_u\boldsymbol{I}\boldsymbol{q}_u \end{aligned} \tag{2b}$$

Spring attachment point locations for a spring j between link u to link v are $\boldsymbol{A}_j$ and $\boldsymbol{B}_j$ respectively. These locations are a linear combination of the proximal joint component

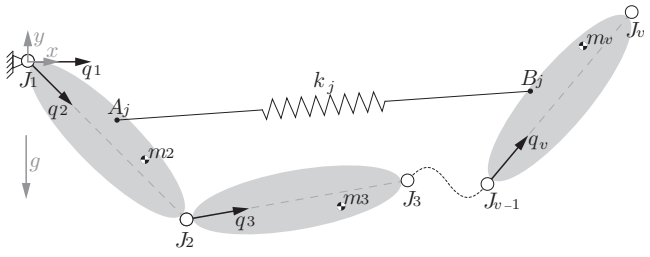

(a)

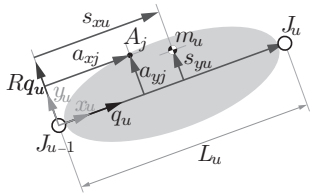

(b)

Fig. 1: (a) Schematic representation of a serial linkage in a state defined by unit vectors $\boldsymbol{q}$. (b) Parameterization of locations on link u in the Cartesian form.

$\boldsymbol{J}_{u-1}$, the local x_u component ($a_{xj}\boldsymbol{I}\boldsymbol{q}_u$) and the local y_u component ($a_{yj}\boldsymbol{R}\boldsymbol{q}_u$) (Eq. 3). A schematic representation containing these components is given in figure 1b.

$$\boldsymbol{A}_j = \boldsymbol{J}_{u-1} + (a_{xj}\boldsymbol{I} + a_{yj}\boldsymbol{R})\,\boldsymbol{q}_u \tag{3a}$$
$$\boldsymbol{B}_j = \boldsymbol{J}_{v-1} + (b_{xj}\boldsymbol{I} + b_{yj}\boldsymbol{R})\,\boldsymbol{q}_v \tag{3b}$$

Similarly the COM location of link u is set up (Eq. 4).

$$\boldsymbol{S}_u = \boldsymbol{J}_{u-1} + (s_{xu}\boldsymbol{I} + s_{yu}\boldsymbol{R})\boldsymbol{q}_u \tag{4}$$

B.2 Step 2: Energy equations and generalized form

This step is to write energy equations in the generalized form, separating the states $\boldsymbol{Q}$ and the parameters in the stiffness matrix $\boldsymbol{K}$.

$$U = \frac{1}{2}\boldsymbol{Q}^T\boldsymbol{K}\boldsymbol{Q} \tag{5}$$

Spring energy is expressed in this form first. The vector describing spring length and orientation for spring j, going from link u to link v, is $\boldsymbol{B}_j - \boldsymbol{A}_j$. This is as a function of the states, because the locations of points $\boldsymbol{B}_j$ and $\boldsymbol{A}_j$ are state dependent as well. The expression for this spring vector is derived in equation 6. An expression is obtained where constants are separated for each state (Eq. 6e). The components $\boldsymbol{C}$ holding these constant parameters are shown in matrix form (Eq. 7).

$$\begin{aligned}\boldsymbol{B}_j - \boldsymbol{A}_j =& \boldsymbol{J}_{v-1} - \boldsymbol{J}_{u-1} - (a_{xj}\boldsymbol{I} + a_{yj}\boldsymbol{R})\,\boldsymbol{q}_u \\ &+ (b_{xj}\boldsymbol{I} + b_{yj}\boldsymbol{R})\,\boldsymbol{q}_v\end{aligned} \tag{6a}$$

$$\begin{aligned}\boldsymbol{J}_{v-1} - \boldsymbol{J}_{u-1} =& \boldsymbol{J}_u + \boldsymbol{J}_{u+1} + \cdots + \boldsymbol{J}_{v-1} \\ =& \sum_{n=u}^{v-1} L_n\boldsymbol{I}\boldsymbol{q}_n\end{aligned} \tag{6b}$$

$$\begin{aligned}\boldsymbol{B}_j - \boldsymbol{A}_j =& -(a_{xj}\boldsymbol{I} + a_{yj}\boldsymbol{R})\,\boldsymbol{q}_u \\ &+ \sum_{n=u}^{v-1} L_n\boldsymbol{I}\boldsymbol{q}_n + (b_{xj}\boldsymbol{I} + b_{yj}\boldsymbol{R})\,\boldsymbol{q}_v\end{aligned} \tag{6c}$$

$$\begin{aligned}\boldsymbol{B}_j - \boldsymbol{A}_j =& \underbrace{((L_u - a_{xj})\boldsymbol{I} - a_{yj}\boldsymbol{R})}_{\boldsymbol{C}_u}\,\boldsymbol{q}_u \\ &+ \underbrace{\sum_{n=u+1}^{v-1} L_n\boldsymbol{I}}_{\boldsymbol{C}_{u+1}+\cdots+\boldsymbol{C}_{v-1}}\,\boldsymbol{q}_n + \underbrace{(b_{xj}\boldsymbol{I} + b_{yj}\boldsymbol{R})}_{\boldsymbol{C}_v}\,\boldsymbol{q}_v\end{aligned} \tag{6d}$$

$$\boldsymbol{B}_j - \boldsymbol{A}_j = \sum_{n=1}^{v} \boldsymbol{C}_n\boldsymbol{q}_n \tag{6e}$$

$$\boldsymbol{C}_u = \begin{bmatrix} L_u - a_{xj} & a_{yj} \\ -a_{yj} & L_u - a_{xj} \end{bmatrix} \tag{7a}$$

$$\boldsymbol{C}_i = \begin{bmatrix} L_i & 0 \\ 0 & L_i \end{bmatrix} \quad \text{, for } i = u+1, \cdots, v-1 \tag{7b}$$

$$\boldsymbol{C}_v = \begin{bmatrix} b_{xj} & -b_{yj} \\ b_{yj} & b_{xj} \end{bmatrix} \tag{7c}$$

$$\boldsymbol{C}_i = \begin{bmatrix} 0 & 0 \\ 0 & 0 \end{bmatrix} \quad \text{, for : } \begin{cases} i = 1, \cdots, u-1 \\ i = v+1, \cdots, n \end{cases} \tag{7d}$$

Knowing the spring length, as a function of the states, its potential energy can be calculated. The equation is set up for a ZFLS j with stiffness k_j (Eq. 8a) and rewritten in the generalized form (Eq. 8d). In this form the states ($\boldsymbol{Q}$) are separated from the parameters in the stiffness matrix of the spring ($\boldsymbol{K}_{s,j}$).

$$U_{s,j} = \frac{1}{2} k_j (\boldsymbol{B}_j - \boldsymbol{A}_j)^2 \tag{8a}$$

$$= \frac{1}{2} k_j \left(\sum_{u=1}^{n} \boldsymbol{C}_u \boldsymbol{q}_u \right)^2 \tag{8b}$$

$$= \frac{1}{2} k_j \begin{bmatrix} \boldsymbol{q}_1 \\ \vdots \\ \boldsymbol{q}_n \end{bmatrix}^T \begin{bmatrix} \boldsymbol{C}_1^T \boldsymbol{C}_1 & \cdots & \boldsymbol{C}_1^T \boldsymbol{C}_n \\ \vdots & \ddots & \vdots \\ \boldsymbol{C}_n^T \boldsymbol{C}_1 & \cdots & \boldsymbol{C}_n^T \boldsymbol{C}_n \end{bmatrix} \begin{bmatrix} \boldsymbol{q}_1 \\ \vdots \\ \boldsymbol{q}_n \end{bmatrix} \tag{8c}$$

$$= \frac{1}{2} \boldsymbol{Q}^T \boldsymbol{K}_{s,j} \boldsymbol{Q} \tag{8d}$$

$$\boldsymbol{K}_{s,j} = k_j \begin{bmatrix} \boldsymbol{C}_1^T \boldsymbol{C}_1 & \cdots & \boldsymbol{C}_1^T \boldsymbol{C}_n \\ \vdots & \ddots & \vdots \\ \boldsymbol{C}_n^T \boldsymbol{C}_1 & \cdots & \boldsymbol{C}_n^T \boldsymbol{C}_n \end{bmatrix} \tag{8e}$$

Next the gravitational energy is expressed in the generalized form of equation 5. The height of the masses is found in the second element of vector $\boldsymbol{S}_u$, containing the global COM y-coordinate of link u. The value for height is extracted by vector product: *height*$= \begin{bmatrix} 0 & 1 \end{bmatrix} \boldsymbol{S}_u$. This product is not jet expressed as in the generalized form because $\boldsymbol{S}_u$ does not contain multiplications of states. By using state $\boldsymbol{q}_1$, which is located on the fixed world, it is known that $(\boldsymbol{R}\boldsymbol{q}_1)^T = \begin{bmatrix} 0 & 1 \end{bmatrix}$, describing the gravitational field direction. Therefore the height of a mass is expressed as in the generalized form by product: *height*$= (\boldsymbol{R}\boldsymbol{q}_1)^T \boldsymbol{S}_u$. Based on this term the energy equations are first written for the mass of a single link u (Eq. 9) followed by a summed relation containing the masses of all links (Eq. 10). For this form the constant components $\boldsymbol{D}_u$ that fill the stiffness matrix are described (Eq. 11), followed by the generalized form of the energy equation (Eq. 12).

$$U_{m_u} = m_u g (\boldsymbol{R}\boldsymbol{q}_1)^T \boldsymbol{S}_u \tag{9a}$$

$$= m_u g \boldsymbol{q}_1^T \boldsymbol{R}^T \boldsymbol{S}_u \tag{9b}$$

$$= m_u g \boldsymbol{q}_1^T \boldsymbol{R}^T \left[\boldsymbol{J}_{u-1} + (s_{xu} \boldsymbol{I} + s_{yu} \boldsymbol{R}) \boldsymbol{q}_u \right] \tag{9c}$$

$$= m_u g \boldsymbol{q}_1^T \boldsymbol{R}^T \left[\sum_{i=1}^{u-1} (L_i \boldsymbol{q}_i) + (s_{xu} \boldsymbol{I} + s_{yu} \boldsymbol{R}) \boldsymbol{q}_u \right] \tag{9d}$$

Effect of combined mass of all links, for a linkage with n links (and thus $n-1$ moving links) is given (Eq. 10).

$$U_{\Sigma m} = \sum_{u=2}^{n} U_{m_u} \tag{10a}$$

$$= \boldsymbol{q}_1^T \sum_{u=2}^{n} \left(\boldsymbol{R}^T m_u g \left[\sum_{i=1}^{u-1} (L_i \boldsymbol{q}_i) + (s_{xu} \boldsymbol{I} + s_{yu} \boldsymbol{R}) \boldsymbol{q}_u \right] \right) \tag{10b}$$

$$= \boldsymbol{q}_1^T \sum_{u=2}^{n} \left(\underbrace{\boldsymbol{R}^T \left[\left(\sum_{i=u+1}^{n} m_i \right) g L_u \boldsymbol{I} + m_u g (s_{xu} \boldsymbol{I} + s_{yu} \boldsymbol{R}) \right]}_{\boldsymbol{D}_u} \boldsymbol{q}_u \right) \tag{10c}$$

$$\boldsymbol{D}_u = \boldsymbol{R}^T \left[\left(\sum_{i=u+1}^{n} m_i \right) g L_u \boldsymbol{I} + m_u g (s_{xu} \boldsymbol{I} + s_{yu} \boldsymbol{R}) \right] \tag{11a}$$

$$= \begin{bmatrix} m_u g s_{yu} & m_u g s_{xu} + \left(\sum_{i=u+1}^{n} m_i \right) g L_u \\ -m_u g s_{xu} - \left(\sum_{i=u+1}^{n} m_i \right) g L_u & m_u g s_{yu} \end{bmatrix} \tag{11b}$$

The generalized form $U_{\Sigma m}$ is obtained as states and parameters are separated.

$$U_{\Sigma m} = \frac{1}{2} \boldsymbol{Q}^T \boldsymbol{K}_m \boldsymbol{Q} \tag{12a}$$

$$\boldsymbol{K}_m = \begin{bmatrix} \boldsymbol{O} & \boldsymbol{D}_2 & \cdots & \boldsymbol{D}_n \\ \boldsymbol{D}_2^T & \boldsymbol{O} & \cdots & \boldsymbol{O} \\ \vdots & \vdots & \ddots & \vdots \\ \boldsymbol{D}_n^T & \boldsymbol{O} & \cdots & \boldsymbol{O} \end{bmatrix} \tag{12b}$$

When analyzing a new system it is possible to quickly set up the stiffness matrices without having to go through all derivations performed in this step. It is advised to directly substitute the component matrices for the springs $\boldsymbol{C}_u$(Eq. 7a-7d) and the mass components $\boldsymbol{D}_u$ (Eq.11). By substituting these component matrices in equation 8e and 12b the stiffness matrix $\boldsymbol{K}_{s,j}$ and $\boldsymbol{K}_m$ are obtained.

B.3 Step 3: Total stiffness matrix

The combined energy U_t, containing all spring and mass terms is obtained by combining the spring and mass stiffness matrices (Eq. 13).

$$U_t = \frac{1}{2} \boldsymbol{Q}^T \boldsymbol{K}_t \boldsymbol{Q} \tag{13a}$$

$$\boldsymbol{K}_t = \left(\sum_{i=1}^{n_{springs}} \boldsymbol{K}_{s,i} \right) + \boldsymbol{K}_m \tag{13b}$$

B.4 Step 4: Constraint equations

In a balanced system, any state can be changed freely with respect to any other state without changing the overall potential energy level. For this to be the case, the effective stiffness between any two different states should be equal to zero. These represent all state dependent energy terms. The effective stiffness terms for these relative rotations are found on the off-diagonal part of the stiffness matrix $\boldsymbol{K}_t$ [14]. As a result, all off-diagonal parts of the $\boldsymbol{K}_t$ matrix are constrained to be equal to zero for balance [13].

The number of constraint equations depends on the size of the $\boldsymbol{K}_t$ matrix, which in turn depends on the number of links n. The matrices are symmetrical, thus all relations are found in the upper triangular part (Eq. 8e, 12b). Additionally, all relations in one of these triangular parts occur twice, once in each even and uneven row. Thus only every other row has to be examined to obtain all relations. Altogether the amount of constraint equations for an n-link system is equal to $n(n-1)$ [14].

B.5 Step 5: Obtain balance by solving constraint equations

The next step is solving the obtained constraint equations. In general, the minimal amount of variables to be calculated is equal to the number of equations. For example, for a three link planar system the number of constraint equations is equal to six and as a result at least six parameters should be left free while solving such a system. The remaining parameters can be selected to have constant values.

III. Application and behavior

In this section an illustrative example of a balanced linkage is presented. The behavior of the balanced system is analyzed to gain a better understanding of how different parameters can be changed while maintaining the desired balance. Increased insight in the inner workings of the system will allow for a more efficient design process and a better overview of possible solutions. Found relations for varying parameters while maintaining balance are provided and visualized. The system studied has two moving links (Figure 2a) and is positioned in a gravitational field acting in the $y-$direction with $g = 9.81m/s^2$.

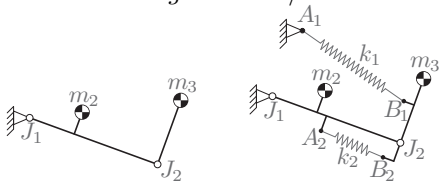

(a) (b)

Fig. 2: (a) Unbalanced linkage. (b) Spring configuration of example 1. (c) Spring configuration of example 2.

A. Example

Two springs are used to balance the system, one bi-articular ZFLS connecting the fixed world to link 3 and one mono-articular ZFLS that connects links 2 and 3 (Figure 2b). In the first step the system locations in figure 2b are expressed in xy-coordinates as in figure 1b. The actual location vectors (Eq. 2,3,4) are not shown as their creation is not required for continuing in this method, nevertheless they are useful for instance to plot the system. In the second step the component matrices for the two springs $\boldsymbol{C}_1$ and $\boldsymbol{C}_2$ (Eq. 14) and the mass terms $\boldsymbol{D}$ (Eq. 15) are constructed based on equations 7 and 11. By substituting these component matrices in equations 8e and 12b the spring matrices $\boldsymbol{K}_{s1}, \boldsymbol{K}_{s2}$ and mass stiffness matrix $\boldsymbol{K}_m$ are obtained (Eq. 16a,16b). The third step is to construct the total stiffness matrix by combining the spring and mass matrices (Eq. 16c). In the fourth step the constraint equations are obtained from the $\boldsymbol{K}_t$ matrix (Eq. 17). The constraint equations to be satisfied for balance are the off-diagonal parts of the $\boldsymbol{K}_t$ matrix set equal to zero. Here only terms in odd rows (1 and 3) are considered as the even rows contain the same relations.

$$\boldsymbol{C}_{1,1} = \begin{bmatrix} -a_{x1} & a_{y1} \\ -a_{y1} & -a_{x1} \end{bmatrix} \quad \boldsymbol{C}_{2,1} = \begin{bmatrix} 0 & 0 \\ 0 & 0 \end{bmatrix}$$
$$\boldsymbol{C}_{1,2} = \begin{bmatrix} L_2 & 0 \\ 0 & L_2 \end{bmatrix} \quad \boldsymbol{C}_{2,2} = \begin{bmatrix} L_2 - a_{x2} & a_{y2} \\ -a_{y2} & L_2 - a_{x2} \end{bmatrix}$$
$$\boldsymbol{C}_{1,3} = \begin{bmatrix} b_{x1} & -b_{y1} \\ b_{y1} & b_{x1} \end{bmatrix} \quad \boldsymbol{C}_{2,3} = \begin{bmatrix} b_{x2} & -b_{y2} \\ b_{y2} & b_{x2} \end{bmatrix} \tag{14}$$

$$\boldsymbol{D}_1 = \begin{bmatrix} 0 & 0 \\ 0 & 0 \end{bmatrix}$$
$$\boldsymbol{D}_2 = \begin{bmatrix} m_2 g s_{y2} & m_3 g L_2 + m_2 g s_{x2} \\ -m_3 g L_2 - m_2 g s_{x2} & m_2 g s_{y2} \end{bmatrix}$$
$$\boldsymbol{D}_3 = \begin{bmatrix} m_3 g s_{y3} & m_3 g s_{x3} \\ -m_3 g s_{x3} & m_3 g s_{y3} \end{bmatrix} \tag{15}$$

$$\boldsymbol{K}_{si} = \frac{1}{2} k_i \begin{bmatrix} \boldsymbol{C}_{i,1}^T \boldsymbol{C}_{i,1} & \boldsymbol{C}_{i,1}^T \boldsymbol{C}_{i,2} & \boldsymbol{C}_{i,1}^T \boldsymbol{C}_{i,3} \\ & \boldsymbol{C}_{i,2}^T \boldsymbol{C}_{i,2} & \boldsymbol{C}_{i,2}^T \boldsymbol{C}_{i,3} \\ \text{sym} & & \boldsymbol{C}_{i,3}^T \boldsymbol{C}_{i,3} \end{bmatrix} \tag{16a}$$
$$\boldsymbol{K}_m = \begin{bmatrix} \boldsymbol{O} & \boldsymbol{D}_2 & \boldsymbol{D}_3 \\ & \boldsymbol{O} & \boldsymbol{O} \\ \text{sym} & & \boldsymbol{O} \end{bmatrix} \tag{16b}$$
$$\boldsymbol{K}_t = \boldsymbol{K}_{s1} + \boldsymbol{K}_{s2} + \boldsymbol{K}_m \tag{16c}$$

$$\boldsymbol{K}_t(1,3) = 0 = -k_1 a_{x1} L_2 + m_2 g s_{y2} \tag{17}$$
$$\boldsymbol{K}_t(1,4) = 0 = -k_1 a_{y1} L_2 + m_2 g s_{x2} + m_3 g L_2$$
$$\boldsymbol{K}_t(1,5) = 0 = -k_1 (a_{x1} b_{x1} + a_{y1} b_{y1}) + m_3 g s_{y3}$$
$$\boldsymbol{K}_t(1,6) = 0 = k_1 (a_{x1} b_{y1} - a_{y1} b_{x1}) + m_3 g s_{x3}$$
$$\boldsymbol{K}_t(3,5) = 0 = k_1 b_{x1} L_2 - k_2 (a_{y2} b_{y2} - b_{x2} (L_2 - a_{x2}))$$
$$\boldsymbol{K}_t(3,6) = 0 = -k_1 b_{y1} L_2 - k_2 (a_{y2} b_{x2} + b_{y2} (L_2 - a_{x2}))$$

In the final step the constraint equations are solved for four different cases, each showing different behavior (Figure 3). Between these cases some general properties of the system remain the same. Specifically spring stiffness, mass and link length values. In each case the constraints are solved for parameters $a_{x1}, b_{x1}, b_{y1}, b_{x2}, b_{y2}$ and k_1. Varied inputs between cases are parameters a_{x2} and a_{y2}, describing the location of attachment A_2. Furthermore s_{y2} is varied, describing the location of the COM of link 2. Obtained parameter values of balanced configurations are summarized in table 3e. Parameters on the first six rows (above the horizontal line) are calculated by solving the constraints, remaining parameter values (under the line) are chosen inputs.

In the first case all spring connections are aligned with the links (Figure 3a). In case 2, attachment A_2 of the second spring is rotated about the joint J_2, as a result attachment B_2 rotates with the same angle about J_2 as well (Figure 3b). In case 3, the COM of link 2 is relocated. Resulting in simultaneous rotations of attachments B_1 and B_2 (Figure 3c). In the final case 4, both offsets of A_2, as in case 2, and s_{y2}, as in case 3, are combined. The solved configuration shows a combination of the behavior caused by the individual offsets of the previous cases (Figure 3d).

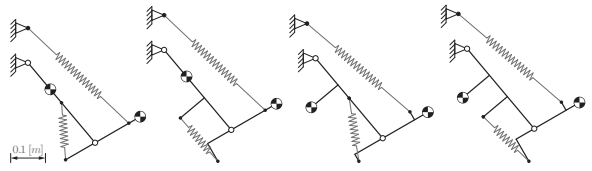

(a) Case 1 (b) Case 2 (c) Case 3 (d) Case 4

	Case 1	Case 2	Case 3	Case 4	Units
a_{x1}	0	0	-0.025	-0.025	$[m]$
b_{x1}	0.1125	0.1125	0.1059	0.1059	$[m]$
b_{y1}	0	0	0.0265	0.0265	$[m]$
b_{x2}	-0.0981	-0.0785	-0.0923	-0.06	$[m]$
b_{y2}	0	-0.0589	-0.0231	-0.0739	$[m]$
k_1	261.6	261.6	261.6	261.6	$[\frac{N}{m}]$
k_2	600	600	600	600	$[\frac{N}{m}]$
a_{y1}	0.1	0.1	0.1	0.1	$[m]$
a_{x2}	0.15	0.18	0.15	0.18	$[m]$
a_{y2}	0	-0.09	0	-0.09	$[m]$
m_2	2	2	2	2	$[kg]$
m_3	2	2	2	2	$[kg]$
L_2	0.3	0.3	0.3	0.3	$[m]$
s_{x2}	0.1	0.1	0.1	0.1	$[m]$
s_{y2}	0	0	-0.1	-0.1	$[m]$
s_{x3}	0.15	0.15	0.15	0.15	$[m]$
s_{y3}	0	0	0	0	$[m]$

(e)

Fig. 3: In scale balanced solutions for example 2. (a) Case 1. (b) Case 2. (c) Case 3. (d) Case 4. (e) Parameter values for the different cases.

B. Behavior in example

The four cases in example 2 are all statically balanced as they all fulfill the constraint equations. The unbalanced three link system is analyzed first in the orientation in which it has minimal gravitational energy (Figure 4a). In this position link 2 is oriented at angle α with respect to the vertical. Angle α is now determined by setting the moment M_{J_1} around J_1 to be equal to zero as it should be when in equilibrium (Eq.18). The system shown in figure 4b is equal to the linkage of figure 4a only with redrawn links that give room for springs to be drawn later on.

$$M_{J_1} = 0 = m_2 s_{y2}\cos(\alpha) - m_2 s_{x2}\sin(\alpha) - m_3 L_2 \sin(\alpha) \tag{18a}$$

$$(m_2 s_{x2} + m_3 L_2)\sin(\alpha) = m_2 s_{y2}\cos(\alpha) \tag{18b}$$

$$\frac{\sin(\alpha)}{\cos(\alpha)} = \tan(\alpha) = \frac{m_2 s_{y2}}{m_2 s_{x2} + m_3 L_2} \tag{18c}$$

$$\alpha = \tan^{-1}\left(\frac{m_2 s_{y2}}{m_2 s_{x2} + m_3 L_2}\right) \tag{18d}$$

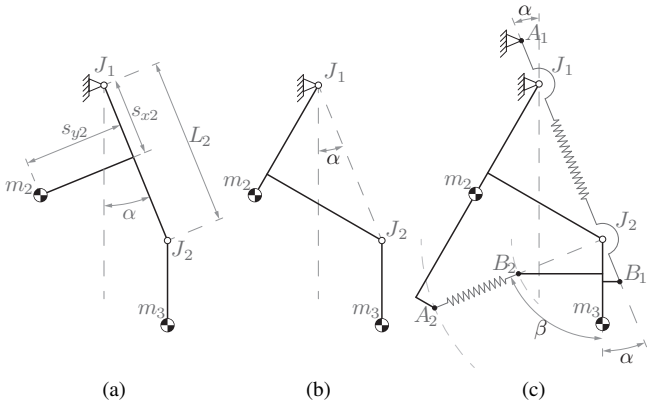

(a) (b) (c)

Fig. 4: (a) and (b) Unbalanced linkage in equilibrium. (c) Relations between the location of spring attachment points required for a balanced system.

Next, it is recognized that for balance a zero moment is required in all orientations. As this is already the case for the original system in the orientation of figure 4b neither of the added springs should apply a moment around any of the joints to keep this moment free condition. Spring 1 is located between the fixed world point A_1 and link 3 at point A_3, and thus spawns both joints. As a result, spring connections A_1 and B_1 should be aligned with both joints J_1 and J_2, exactly at the previously determined angle α (Figure 4c). Spring 2 connects A_2 on link 2 and B_2 on link 3 and thus spawns only the second joint J_2. Therefore, in this orientation with minimal potential the two connection points of this spring are to be aligned with J_2 (Figure 4c).

Furthermore, as α is only dependent on parameters of the original linkage its value is unaffected by adjusting the other spring. For spring 2 the alignment of attachment A_2

depends on both angles α and β with respect to the local coordinate system of link 2. Attachment B_2 is dependent only on angle β with respect to the local coordinates of links 3. Therefore, by changing β spring 2 can be relocated anywhere on a ring shaped disk around J_2, as partially visualized by dotted lines in figure 4c.

The locations of the spring attachments are now described based on a single position of the linkage where the gravitational energy is at a minimum. This does not directly prove that the system is in balance in any pose as it is only clear that this one position is in equilibrium. However, the proof that the system can be balanced in any configuration is already given using the stiffness matrix approach. What the analysis of this single position does provide is insight in where the attachments can be placed and why they are constrained to lie on certain lines or positions. Additionally it can be reasoned that the system is capable of being balanced in all orientations as the energy behavior of all components is sinusoidal with respect to each rotation. These sinusoids have equal periods as these are equivalent to full rotations of a links, all having a minimum or maximum in the orientation of figure 4. The sinusoidal functions are either in phase or shifted by half a phase exactly and so can interfere with one another to cancel each other out.

The behavior described so far in this example is based on the orientations in which springs can be placed for the selected spring configuration (Figure 4). However some additional interesting observations are made based on parameter magnitudes.

The first observation is that the location of spring attachment point B_1 (Figure 4c) is a unique point depending solely on parameters of the original linkage, i.e. it is fixed independently of all other spring related parameters. Using the `solve` function in MATLAB the constraint equations are solved for parameters b_{x1} and b_{x2}. These parameters describe the location of B_1, expressed as a function of the other parameters (Eq.19). The obtained equations consist solely of parameters describing link length, mass or COM location. Thus, the location of this attachment point can not be varied when the linkage that is to be balanced has fixed dimensions and mass.

$$b_{x1} = \frac{L_2^2 m_3^2 s_{x3} + L_2 m_2 m_3 (s_{x2} s_{x3} + s_{y2} s_{y3})}{(L_2 m_3 + m_2 s_{x2})^2 + m_2^2 s_{y2}^2} \tag{19a}$$

$$b_{y1} = \frac{L_2^2 m_3^2 s_{y3} + L_2 m_2 m_3 (s_{x2} s_{y3} - s_{x3} s_{y2})}{(L_2 m_3 + m_2 s_{x2})^2 + m_2^2 s_{y2}^2} \tag{19b}$$

For the spring attachment A_1 an additional constraint is found. It is found that the distance from joint J_1 to this point A_1 is inversely related to its spring stiffness k_1. This is by solving the constraint equations (Eq.17) for the parameters a_{x1} and a_{y1} which describe the location of A_1 (Eq.20a and 20b). Furthermore, the relation for α can again be extracted from these constraints by looking at the relative magnitudes of a_{x1} and a_{y1} (Eq.20c).

$$a_{x1} = \frac{m_2 g s_{y2}}{L_2} \frac{1}{k_1} \tag{20a}$$

$$a_{y1} = \frac{m_2 g s_{x2} + m_3 g L_2}{L_2} \frac{1}{k_1} \tag{20b}$$

$$\alpha = \tan^{-1}\left(\frac{a_{x1}}{a_{y1}}\right) = \tan^{-1}\left(\frac{m_2 s_{y2}}{m_2 s_{x2} + m_3 L_2}\right) \tag{20c}$$

For spring 2, an additional constraint is found as well, this is next to angle β which describes the springs orientation. When all other parameters are fixed, the product of its stiffness k_2, distance from J_2 to A_2 and distance from J_2 to B_2 is constant ($k_2 \cdot |A_2 - J_2| \cdot |B_2 - J_2| =$ constant). In other words, the two described lengths and the stiffness of this spring can be varied freely within these bounds without affecting any other parameter. This magnitude of the 'constant' value in this relation is affected by the location of A_1 and k_1, however it is unpractical to take these into account in the same relation and much more convenient to fix these parameters before altering either A_2, B_2 or k_2.

IV. Discussion

Constraint equations in polar form, for the system studied in the presented example, are set up in the work of Lin et al.[13]. In this form link locations are defined by a magnitude and an angle, representing the same relations as in equation 17. Behavior found in the presented example shows a number of simultaneous rotations of COM locations and/or spring connection points that can be performed without affecting the balance of the system (Figure 4). One could argue to use a polar coordinate system to describe this behavior as it is rotational. However, the centers of rotation for these simultaneous rotations can either be on the first joint, the second joint or a seemingly arbitrary point on one of the links. As the location of the center point is inconsistent it cannot be ensured that this point is always positioned on the origin of the local coordinate system from which the polar coordinates are defined. Furthermore, describing a rotation using polar coordinates about a point other than the origin is, according to the authors, unnecessarily complicated compared to describing such a rotation as a sum of vector components in a Cartesian coordinate system. Moreover, using polar coordinates the possibility of this rotational behavior is not recognized in literature [15]. Criteria are set which limit spring attachment to be on fixed lines instead of allowing planar placement [15]. As the Cartesian design equations describe the balance conditions in a simpler manner it is easier to find solutions in the complete design space using these coordinates. For this reason a Cartesian coordinate system is recommended when altering a system having planar offsets. Other benefits of using a Cartesian system are that the resulting constraint equations will be free of sinusoidal term, and describing coordinates

on a link using xy-components is more intuitive compared to using an angle and magnitude.

V. Conclusion

In this work the implementation of the stiffness matrix approach is altered such that states and link locations are expressed in the same coordinate system. The first goal was to implement Cartesian coordinates and comparing it to the use of polar coordinates in the stiffness matrix approach. The Cartesian coordinates were successfully implemented and in comparison they were found to be more intuitive in use, provide simpler constraint equations and be more convenient for altering parameters of balanced systems. The main benefit of this simpler description is that previously unidentified solutions, having planar spring attachment placement, are now recognized. The second goal was to gain more insight in the relations between parameters while the third goal was to illustrate these behavioral relations in two examples. These two goals were achieved simultaneously as in the example a basic system (having two moving links) was analyzed. Relations were found between orientation, positioning and magnitude of springs and masses. These are described and illustrated providing a visual overview of the design space. Obtained relations provide knowledge in the possibilities to vary spring system parameters while maintaining static balance.

VI. Acknowledgments

This research is part of the project 'Flextension', sponsored by Technology Foundation STW, project 11832.

References

[1] J. L. Herder, Energy-free systems; theory, conception and design of statically balanced spring mechanisms, Ph.d. thesis, Delft University of Technology, iSBN 90-370-0192-0 (2001).

[2] S. K. Agrawal, A. Fattah, Gravity-balancing of spatial robotic manipulators, Mechanism and machine theory 39 (12) (2004) 1331–1344.

[3] A. H. Stienen, E. E. Hekman, G. B. Prange, M. J. Jannink, F. C. van der Helm, H. van der Kooij, Freebal: design of a dedicated weight-support system for upper-extremity rehabilitation, Journal of Medical Devices 3 (4) (2009) 041009.

[4] M. Carricato, C. Gosselin, A statically balanced gough/stewart-type platform: conception, design, and simulation, Journal of Mechanisms and Robotics 1 (3) (2009) 031005.

[5] K. Kobayashi, Comparison between spring balancer and gravity balancer in inertia force and performance, Journal of Mechanical Design 123 (4) (2001) 549–555.

[6] G. Endo, H. Yamada, A. Yajima, M. Ogata, S. Hirose, A passive weight compensation mechanism with a non-circular pulley and a spring, in: Robotics and Automation (ICRA), 2010 IEEE International Conference on, IEEE, 2010, pp. 3843–3848.

[7] C.-W. Hou, C.-C. Lan, Functional joint mechanisms with constant-torque outputs, Mechanism and Machine Theory 62 (2013) 166–181.

[8] R. Sapper, Lamp with an articulated support, uS Patent 3,790,773 (Feb. 5 1974).

[9] J. Wang, C. M. Gosselin, Static balancing of spatial three-degree-of-freedom parallel mechanisms, Mechanism and Machine Theory 34 (3) (1999) 437–452.

[10] H. Hilpert, Weight balancing of precision mechanical instruments, Journal of Mechanisms 3 (4) (1968) 289 – 302.

[11] S. K. Banala, S. K. Agrawal, A. Fattah, V. Krishnamoorthy, H. Wei-Li, J. Scholz, K. Rudolph, Gravity-balancing leg orthosis and its performance evaluation, Robotics, IEEE Transactions on 22 (6) (2006) 1228–1239.

[12] P.-Y. Lin, W.-B. Shieh, D.-Z. Chen, A theoretical study of weight-balanced mechanisms for design of spring assistive mobile arm support (mas), Mechanism and Machine Theory 61 (2013) 156–167.

[13] P.-Y. Lin, W.-B. Shieh, D.-Z. Chen, A stiffness matrix approach for the design of statically balanced planar articulated manipulators, Mechanism and Machine Theory 45 (12) (2010) 1877–1891.

[14] P.-Y. Lin, W.-B. Shieh, D.-Z. Chen, Design of statically balanced planar articulated manipulators with spring suspension, Robotics, IEEE Transactions on 28 (1) (2012) 12–21.

[15] Y.-Y. Lee, D.-Z. Chen, Determination of spring installation configuration on statically balanced planar articulated manipulators, Mechanism and Machine Theory 74 (2014) 319–336.

[16] S. R. Deepak, G. Ananthasuresh, Perfect static balance of linkages by addition of springs but not auxiliary bodies, Journal of Mechanisms and Robotics 4 (2) (2012) 021014.